6-6-2007

The Stability of Al11Sm3 (Al4Sm) Phases in the Al-Sm Binary System

Shihuai Zhou
Iowa State University, szhou@ameslab.gov

Ralph E. Napolitano
Iowa State University, ren1@iastate.edu

The Stability of Al11Sm3 (Al4Sm) Phases in the Al-Sm Binary System

Abstract
The relative stability of $Al_{11}Sm_3$ (Al_4Sm) intermetallic phases was experimentally investigated through a series of heat treatments followed by microstructural, microchemical, and X-ray diffraction (XRD) analyses. The principal findings are that the high-temperature tetragonal phase is stable from 1655 to 1333 K and that the low-temperature orthorhombic phases, α and γ, have no range of full stability but are metastable with respect to the crystalline Al and Sm reference states down to 0 K. Thermodynamic modeling is used to describe the relative energetics of stable and metastable phases along with the associated two-phase mixtures. Issues regarding transition energetics and kinetics are discussed.

Keywords
Ames Laboratory, Materials and Engineering Physics

Disciplines
Metallurgy

Comments
This article is from *Metallurgical and Materials Transactions A* 38 (2007): 1145, doi:10.1007/s11661-007-9148-z. Posted with permission.

The Stability of $Al_{11}Sm_3$ (Al_4Sm) Phases in the Al-Sm Binary System

S.H. ZHOU and R.E. NAPOLITANO

The relative stability of $Al_{11}Sm_3$ (Al_4Sm) intermetallic phases was experimentally investigated through a series of heat treatments followed by microstructural, microchemical, and X-ray diffraction (XRD) analyses. The principal findings are that the high-temperature tetragonal phase is stable from 1655 to 1333 K and that the low-temperature orthorhombic phases, α and γ, have no range of full stability but are metastable with respect to the crystalline Al and Sm reference states down to 0 K. Thermodynamic modeling is used to describe the relative energetics of stable and metastable phases along with the associated two-phase mixtures. Issues regarding transition energetics and kinetics are discussed.

DOI: 10.1007/s11661-007-9148-z

I. INTRODUCTION

THE formation of crystalline phases in aluminum–rare-earth (Al-RE) binary alloys has received considerable attention due to a number of interesting phenomena related to rapid solidification,[1] glass formation,[2,3] devitrification behavior,[4] and nanocrystalline applications.[5,6] In this work, we focus on the binary Al-Sm system, a glass forming system that exhibits a wider amorphous composition range than many other Al-RE alloys and a number of intermetallic crystalline phases whose relative stability has been difficult to assess.[7,8,9] Accordingly, we employ X-ray diffraction (XRD) and electron beam microanalysis methods to examine the stability of several phases with the $Al_{11}Sm_3$ (or Al_4Sm) stoichiometry and consider the implications with respect to this portion of the equilibrium phase diagram and reported devitrification sequences.

The first reports of stable Al-Sm intermetallic phases are attributed to Iandelli[10] and to Wernick and Geller,[11] but the first detailed and systematic study of this system was reported by Buschow and van Vucht,[7] who used microscopy as well as thermoanalytical and XRD methods to identify ranges of stability, crystal structure, and lattice parameters for intermetallic phases of Al_4Sm, Al_3Sm, Al_2Sm, AlSm, and $AlSm_2$ stoichiometries. The results of Buschow and van Vucht[7] were subsequently supported by the work of Casteels,[12] with several minor refinements of stability ranges and lattice parameters.*

*We note here that neither Bushow and Vucht nor Casteels was able to corroborate Iandella's finding that an intermetallic $AlSm_3$ phase is stable over some temperature range.

Both of these reports also indicate that the tetragonal Al_4Sm (β) phase melts congruently at about 1723 K and decomposes catatectically to liquid plus Al_3Sm (δ) on cooling at approximately 1351 K (Table I provides the phase symbols used throughout this article). The observation that this phase "melts on cooling" was significant in that it was notably different from analogous Al_4RE phases in other Al-RE binary systems (*e.g.*, Al_4La, Al_4Ce, Al_4Pr, Al_4Nd, and Al_4Pm), each of which exhibits a tetragonal to orthorhombic transition with no decomposition.[13] Examining this issue, Buschow and van Vucht reported that the low-temperature α phase was observed in one instance after repeated temperature cycling of a 0.25 at. pct Sm sample, but that it was not reproducible, concluding that the α phase is metastable[13,14] and that it may be stabilized by impurities. With this issue of α phase stability remaining unresolved, subsequently reported phase diagrams continued to show the catatectic decomposition of the β phase.[15,16] More recently, Saccone *et al.*[9] used a CALPHAD approach to compute the Al-Sm phase diagram and, because there was no clear experimental basis for determining the relative stability of the α phase, accounted for both situations, where the β phase may (1) decompose catatectically to L + δ or (2) transform allotropically to the orthorhombic α phase.[9] The latter case is shown in Figure 1, and a summary of observed phases and phase stability reports is given in Table I.

In addition to the unresolved thermodynamic issues, experimental reports of crystal formation in this system involving both solidification from the melt and the devitrification of amorphous alloys are equally unclear.

S.H. ZHOU, Assistant Scientist, is with the Materials & Engineering Physics Program, Ames Laboratory, United States Department of Energy. R.E. NAPOLITANO, Associate Professor, Materials & Engineering Physics Program, Ames Laboratory, is with the Department of Materials Science and Engineering, Iowa State University, Ames, IA 50011, USA. Contact e-mail: ralphn@iastate.edu
Manuscript submitted November 28, 2006.
Article published online June 6, 2007.

Table I. A Summary of Crystalline Phases Reported in the Binary Al-Sm System

Stoichio-metry	Prototype	Structure	Symbol in Fig. 1	No.	First Principles ΔH (kJ/mol)	Reported as		
						Stable	Metastable	Observed
Al	Cu	cubic (A1)	fcc	225	0	7,12,13	—	8,18
$Al_{11}Sm_3$-α	$Al_{11}La_3$-α	orthorhombic	α	71	–31.68	23	—	7,13
Al_4Sm-β	Al_4Ba	tetragonal	β	139	–28.09	7,12,13	—	8,18
Al_4Sm-γ	Al_4U	orthorhombic	γ	74	–15.80	—	12	8,18
Al_3Sm	Ni_3Sn	hexagonal ($D0_{19}$)	δ	194	—	7,10,12,13	—	—
~Al_3Sm	Al_6DyV	hexagonal	ε	—	—	—	—	8,18
?	—	cubic	φ	—	—	—	—	18
?	—	cubic	η	—	—	—	—	8,18
Al_2Sm	Cu_2Mg	cubic (C15)	σ	227	—	7,10–13	—	—
AlSm	AlEr	orthorhombic	θ	57	—	7,13	—	—
$AlSm_2$	Co_2Si	orthorhombic(C23)	χ	62	—	7,13	—	—
Sm	αSm	trigonal (C19)	rho	166	0	7,12,13	—	—
Amorphous	—	—	A	—	—	—	8,18	—

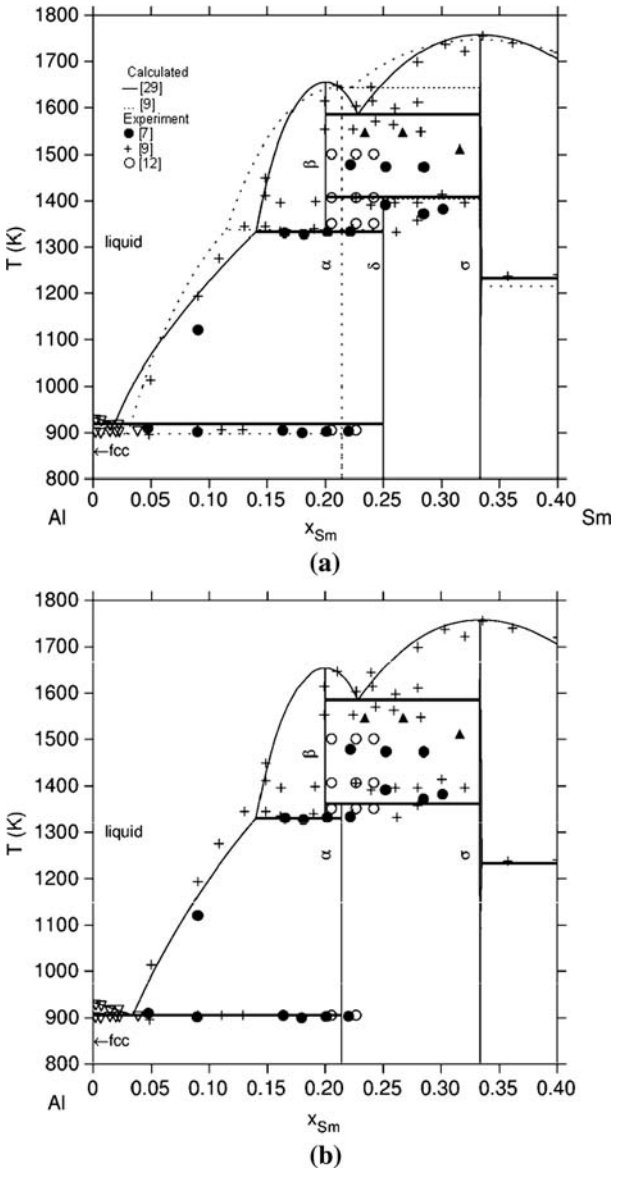

Fig. 1—(*a*) Al-Sm phase diagram. (*b*) The metastable Al-Sm phase diagram (with the δ phase suppressed).

Rizzi *et al.*[17] investigated Al-Sm melt-spun ribbons, showing that either β or fcc-Al may nucleate and grow from the alloy (8 to 12 at. pct Sm) melt. Guo *et al.*[8] examined crystallization in amorphous Al-Sm melt-spun ribbons (8 to 14 at. pct Sm), employing 1-h (3600-s) low-temperature (< 900 K) annealing treatments, reporting the following general isothermal crystallization sequences:

$$(8 \text{ at. pct Sm}) \quad A \rightarrow A + \text{fcc} \rightarrow \text{fcc} + \beta \rightarrow \text{fcc} + \gamma$$

$$(10/12 \text{ at. pct Sm}) \quad A \rightarrow \text{fcc} + \beta + \varepsilon \rightarrow \text{fcc} + \gamma$$

and

$$(14 \text{ at. pct Sm}) \quad A \rightarrow \text{fcc} + \beta + \eta \rightarrow \text{fcc} + \beta + \varepsilon \rightarrow \text{fcc} + \gamma$$

A similar investigation of Al-8 at. pct Sm was performed by Rizzi *et al.*,[18] who found that η does not form from the glass and observed two different devitrification sequences, depending on whether any of the η phase had nucleated from the melt:

$$(1) \quad A \rightarrow \phi \rightarrow \text{fcc} + \beta + \varepsilon \rightarrow \text{fcc} + \gamma$$

and

$$(2) \quad A + \text{fcc} + \eta \rightarrow A + \text{fcc} + \beta \rightarrow \text{fcc} + \gamma$$

Wilde *et al.*[19] used glassy alloys produced by ambient temperature mechanical alloying of Al-8 at. pct Sm specimens to investigate the glass transition temperature (T_g = 445 K[19]) and crystallization. In that experiment, it was observed that formation of a metastable Al_4Sm phase (not identified as β or γ) preceded the formation of the equilibrium Al and δ phases during heat treating between T_g (445 K) and 503 K.

While these and other experimental reports [7,8,12,13,18,20–23] indicate that β is stable at high temperature (~1339 to 1723 K) and metastable at low temperature (below ~1339 K), the relative stability of the orthorhombic α and γ phases at low temperature is unclear, and the question as to whether these phases have any range of full stability

remains outstanding. It is in this vane that the current investigation into the relative stabilities of the compounds α, β, and γ is primarily motivated. In addition, an understanding of the complex devitrification sequences observed in this system requires accurate quantification of the relevant energetics.

Our approach is to investigate the phase stability by combining isothermal heat treatments followed by X-ray and electron-beam microanalysis with first principle and solution-based thermodynamic calculations to quantify the relative stability of the α, β, and γ phases and the respective equilibria between these phases, the alloy liquid, and the relevant competing two-phase mixtures. For our experiments, we employ a test alloy composition of Al-18 at. pct Sm and perform heat treatments between 973 and 1373 K, where we investigate equilibrium between the liquid phase and the various stable or metastable solid phases.

II. EXPERIMENTS

Alloy test specimens of Al-18 at. pct Sm were prepared by arc melting the pure elements (0.99999 Al and 0.999 Sm, by weight[24]) on a copper hearth in an argon atmosphere. Each alloy specimen, of approximately 15 grams, was arc melted 3 times to ensure homogeneity, placed in a closed graphite crucible, and sealed in quartz under an argon atmosphere. Specimens were heat treated using the temperature/time combinations listed in Table II and quenched in water to room temperature. Both as-cast and heat-treated specimens were characterized using XRD with Cu K_α radiation, scanning electron microscopy (SEM) with energy-dispersive spectroscopy (EDS), and electron probe microanalysis (EPMA) with wavelength dispersive spectroscopy (20 kV, ~10 nA).

The typical microstructure for the as-arc-melted Al-18 at. pct Sm test alloy is shown in Figure 2(a). This microstructure is comprised of a large fraction of primary globular α phase, surrounded by an interglobular eutectic constituent of α plus fcc-Al, as indicated by the (0-hours) XRD results, as shown in Figure 3 and listed in Table II. The EDS and EPMA microchemical analyses, summarized in Table II, indicate an α phase composition of $x^{\alpha}_{Sm} = 0.203$, which deviates somewhat from the composition $x^{\alpha}_{Sm} = 0.214$ suggested by Buschow and van Vucht[13] and proposed by Saccone *et al.*[9] While our experimentally determined value of x^{α}_{Sm} may be taken to suggest an Al_4Sm stoichiometry, we point out that our X-ray measurements clearly indicate the orthorhombic structure of the $Al_{11}La_3$ prototype. We note here that a similar contradiction was addressed by Gomes de Mesquita *et al.*,[14] who reported that the low-temperature orthorhombic phase (α) has the stoichiometry of $Al_{11}Sm_3$ and asserted that the β phase most likely exhibits this stoichiometry as well, even though it exhibits the tetragonal structure of the Al_4Ba type. Buschow and van Vucht[13] reconciled this issue by surmising that the high-temperature phase (β) maintains a tetragonal structure, where one-twelfth of the aluminum sites are vacant. Thus, they argue that vacancy ordering is an essential feature of the β-to-α transition.

Phase composition measurements for the major phase in heat-treated specimens are also summarized in Table II, where each listed composition is an average of ten measurements. For a temperature of 1173 K, we observed that the α phase decomposition is very sluggish, where the XRD data (Figure 3) indicate that the δ phase takes between 21 and 25 hours to form at this temperature, consistent with the microstructures shown in Figures 2(b) and (c). In specimens heated for 25 and 46 hours, shown in Figures 2(c) and (d), the composition of the intermetallic phase was measured to be 0.252 and 0.253, respectively (Table II), further supporting the X-ray data, again indicating that the $\alpha \rightarrow L + \delta$ transition had already occurred.

Microstructural (Figure 4), chemical (Table II), and X-ray (Figure 5) analyses from similar experiments involving heat treatment temperatures ranging from 973 to 1293 K confirm the relative stability of the $L + \delta$ mixture over that of the α phase throughout this temperature range. An upper limit to the stability of the δ phase is indicated by the experimental result obtained after heating to 1373 K for 25 hours, where we observe only β in equilibrium with the liquid phase

Table II. Major Phase Identification and Composition Measurements (± 0.025) for Al-18 At. Pct Sm after the Indicated Heat Treatment

		Annealing Time, Hours							
T (K)		0	5	10	20	21	22	25	46
973	x_{Sm}	0.204 α	—	—	0.249	—	0.251	—	—
	phase		—	—	δ	—	δ	—	—
1073	x_{Sm}		—	0.203	0.215	—	—	—	—
	phase		—	α	α	—	—	—	—
1173	x_{Sm}		0.209	—	—	0.203	—	0.253	0.252
	phase		α	—	—	α	—	δ	δ
1273	x_{Sm}		—	0.251	—	—	—	—	—
	phase		—	δ	—	—	—	—	—
1293	x_{Sm}		—	—	—	—	0.258	—	—
	phase		—	—	—	—	δ	—	—
1373	x_{Sm}		—	—	—	—	—	0.202	—
	phase		—	—	—	—	—	β	—

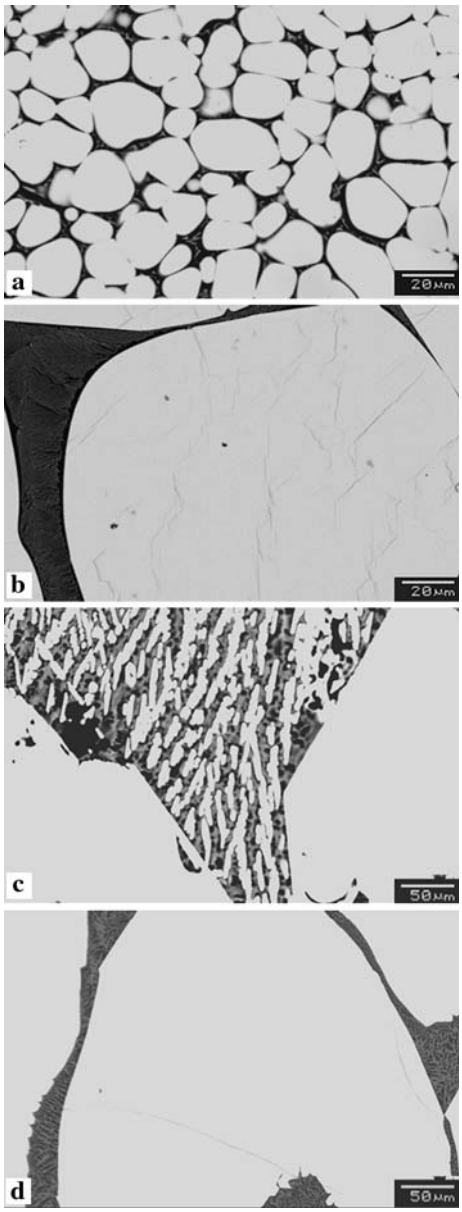

Fig. 2—SEM images showing observed microstructures after heat treating the as-arc-melted Al-18 at. pct Sm alloy at 1173 K for (*a*) 0 h, (*b*) 21 h, (*c*) 25 h, and (*d*) 46 h (each followed by water quenching).

(upper trace in Figure 5). This finding is consistent with the observations of Buschow *et al.*[7,13] and Casteels *et al.*,[12] from which they conclude that the β phase is stable at high temperatures (above 1321 and 1351 K, respectively) up to its melting point at 1663 K.

III. FIRST-PRINCIPAL CALCULATIONS

To clarify the low-temperature stabilities of the compounds α, β, and γ, we compute the associated zero-Kelvin enthalpies of formation using a first-principles approach. The total energy of these phases, along with the Al (fcc) and Sm (rhombohedral) references, are

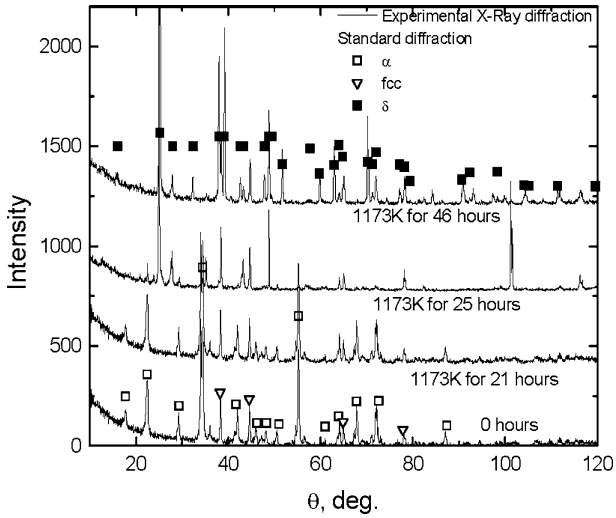

Fig. 3—XRD data for the alloys shown in Fig. 2.

computed using the VASP[25] code with Vanderbilt ultrasoft pseudopotentials[26] (Monkhost $12 \times 12 \times 12$ k points with the high precision generalized gradient approximation[27]). Relaxation of the β and γ phases was performed only with respect to specific volume, due to the limited stability of these intermetallic compounds. For the α phase, however, full relaxation with respect to unit cell volume, shape, and internal atomic coordinates was possible, do to its greater low-temperature stability.

The enthalpy of formation (ΔH_f) for a given compound is calculated as the difference between the energy (E) of the compound and linear combination of the pure element reference state energies,

$$\Delta H_{\mathrm{f}} = E - x_{\mathrm{Al}} E_{\mathrm{Al}}^{\mathrm{fcc}} - x_{\mathrm{Sm}} E_{\mathrm{Sm}}^{\mathrm{rho}}$$

The results, summarized in Table I, indicate that α, β, and γ intermetallic phases have a negative zero-Kelvin energy with the α phase being the most stable among them. The Gibbs free energies of these phases at non-zero temperatures will be discussed in Section IV.

IV. DISCUSSION

The experimental data and first principles calculations described in the preceding sections indicate relative phase stability at various specific conditions. To address more generally the stability of the intermetallic phases, particularly the $Al_{11}Sm_3$ (α) and Al_4Sm (β, γ) phases, we employ a solution thermodynamics formulation, where we describe the free energy of the general Al_pSm_q compound as

$$\begin{aligned} {}^{\circ}G_{\mathrm{Al}_p\mathrm{Sm}_q} &= p\,{}^{\circ}G_{\mathrm{Al}}^{\mathrm{fcc}} + q\,{}^{\circ}G_{\mathrm{Sm}}^{\mathrm{rho}} + \Delta G_{\mathrm{Al}_p\mathrm{Sm}_q} \\ &= p\,{}^{\circ}G_{\mathrm{Al}}^{\mathrm{fcc}} + q\,{}^{\circ}G_{\mathrm{Sm}}^{\mathrm{rho}} + a_{\mathrm{Al}_p\mathrm{Sm}_q} + b_{\mathrm{Al}_p\mathrm{Sm}_q} T \end{aligned}$$

where ${}^{\circ}G_{\mathrm{Al}}^{\mathrm{fcc}}$ and ${}^{\circ}G_{\mathrm{Sm}}^{\mathrm{rho}}$ are the molar Gibbs free energies for Al(fcc) and Sm(rho),[28] respectively. The details of the comprehensive treatment of the Al-Sm binary system are described elsewhere,[29] but we use

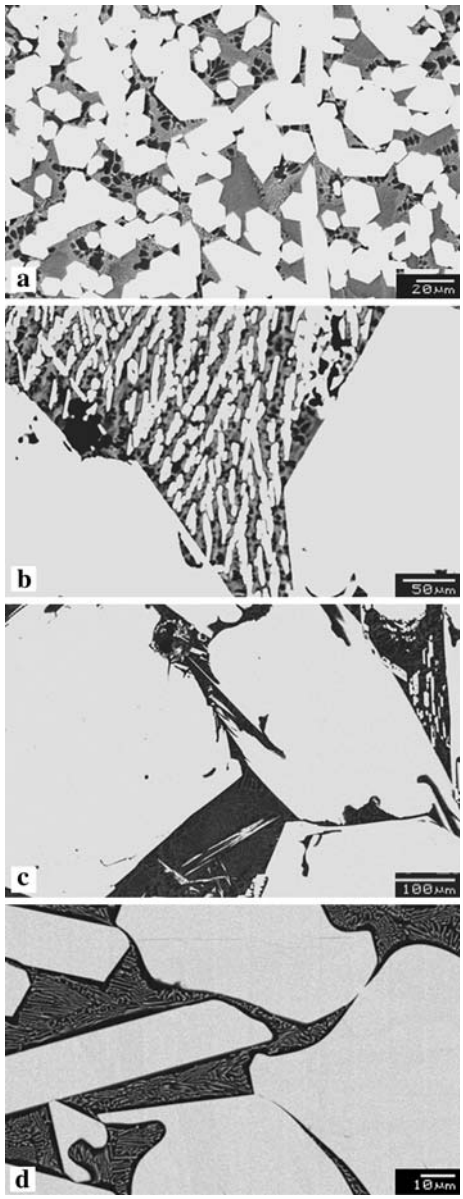

Fig. 4—SEM images showing observed microstructures after heat treating the as-arc-melted Al-18 at. pct Sm alloy at (*a*) 973 K for 22 h, (*b*) 1173 K for 25 h, (*c*) 1293 K for 22 h, and (d) 1373 K for 25 h (each followed by water quenching).

the model parameters, $a_{\mathrm{Al}_p\mathrm{Sm}_q}$ and $b_{\mathrm{Al}_p\mathrm{Sm}_q}$, for both the compound and liquid phases,[29] as listed in Table III, to model the binary phase diagram, as shown in Figure 1. Figure 1(a) shows that the δ phase is a stable phase and that the δ liquidus is the relevant equilibrium liquidus from 919 to 1333 K. Figure 1(b) shows the calculated phase diagram, constrained to exclude the δ phase. This diagram exhibits the metastable α liquidus between 906 and 1320 K, indicating that the α phase is favored over the σ phase and that the L + α equilibrium becomes relevant if the δ phase is suppressed. This is consistent with our observation of primary α in the as-cast specimens (Table I).

In Figure 6 (a), we directly compare the stability of the various phases at $x_{\mathrm{Sm}} = 0.2$ by plotting the Gibbs free

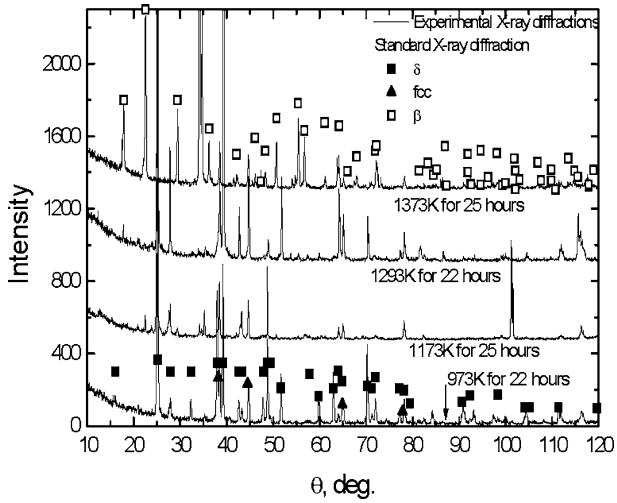

Fig. 5—XRD data for the alloys shown in Fig. 4.

Table III. Thermodynamic Parameters for the Al-Sm System[29]

Phase	Parameter	Value (J/mol)
Liquid	${}^0L^{\mathrm{liq}}_{\mathrm{Al,Sm}}$	−80,524
	${}^0L^{\mathrm{liq}}_{\mathrm{Al,Al_2Sm_1}}$	−26,012
	${}^0L^{\mathrm{liq}}_{\mathrm{Al_2Sm_1,Sm}}$	−42,022
	$\Delta G^0_{\mathrm{Al_2Sm_1}}$	−144,212 + 35.854 T
Al_4Sm-β	$\Delta G^{\beta}_{\mathrm{Al:Sm}}$	−23,121 - 6.202 T
$Al_{11}Sm_3$-α	$\Delta G^{\alpha}_{\mathrm{Al:Al}}$	21,708
	$\Delta G^{\alpha}_{\mathrm{Al:Sm}}$	−34,800 + 1.344 T
	$\Delta G^{\alpha}_{\mathrm{Sm:Al}}$	31,451.8
	$\Delta G^{\alpha}_{\mathrm{Sm:Sm}}$	27,555.6
Al_4Sm-γ	$\Delta G^{\gamma}_{\mathrm{Al:Sm}}$	−28,535
Al_3Sm-$D0_{19}$	$\Delta G^{\mathrm{D0_{19}}}_{\mathrm{Al:Sm}}$	−48,386 + 8.342 T
Al_2Sm-C_{15}	$\Delta G^{\mathrm{C15}}_{\mathrm{Al:Sm}}$	−55,000 + 7.382 T

energies of α, β, and γ, with respect to the liquid phase, over the full range of relevant temperatures. In this plot, we also include the Gibbs free energies for the δ + Al(fcc) and δ + liquid two-phase mixtures, associated with the Al_4Sm composition, and we identify the relevant transitions involving stable or metastable phases. The progression (on cooling) of stable phases is identified as L $\rightarrow$ β $\rightarrow$ L + δ $\rightarrow$ δ + Al(fcc). The plot also shows clearly that the equilibrium phase diagram should include the β-L-δ invariant, indicating a β $\rightarrow$ L + δ decomposition on cooling through 1333 K, as compared with experimental reports of 1321[7,13] and 1351 K.[12] Figure 6(a) also shows that the β phase, which may grow either from an undercooled melt or from an amorphous solid, is metastable below 1333 K, and, therefore, may transform into either α (below 1135 K) or γ (below 873 K). This is consistent with the reports of Guo *et al.*[8] and Rizzi *et al.*,[18] where γ formation was observed to follow β formation in the devitrification of amorphous ribbons. In Figure 6(b), we plot the Gibbs free energy of the liquid and β phases and compare them to the Gibbs free energy of the three

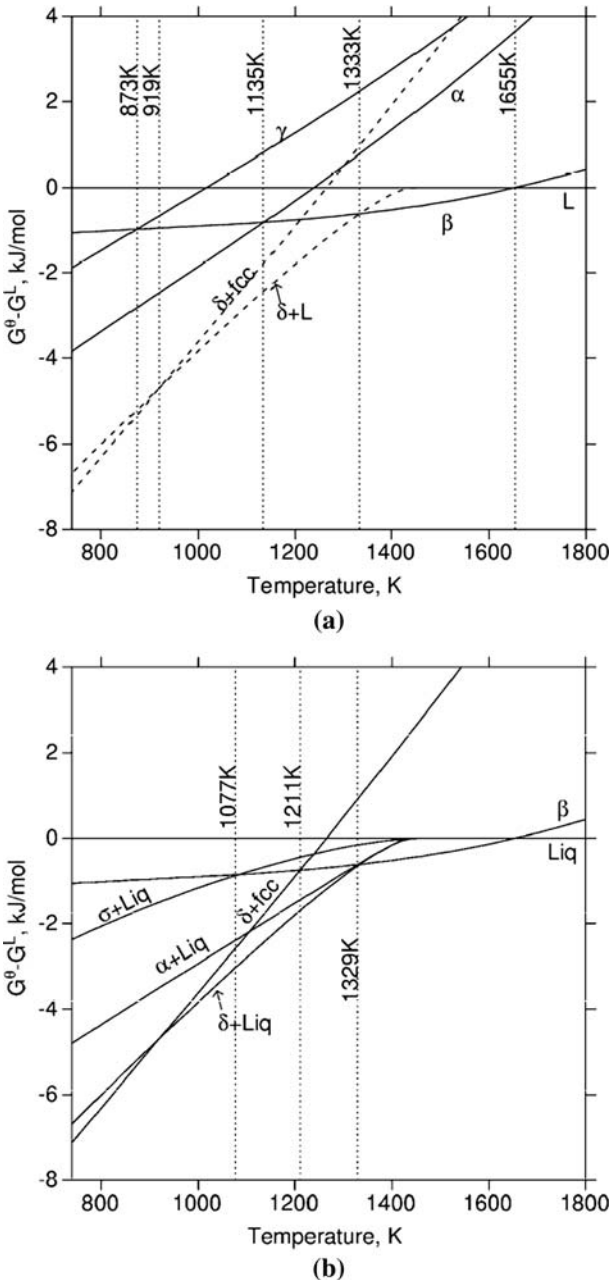

Fig. 6—Gibbs free energy for the Al_4Sm phases and the relevant two-phase mixtures, computed with respect to the liquid phase.

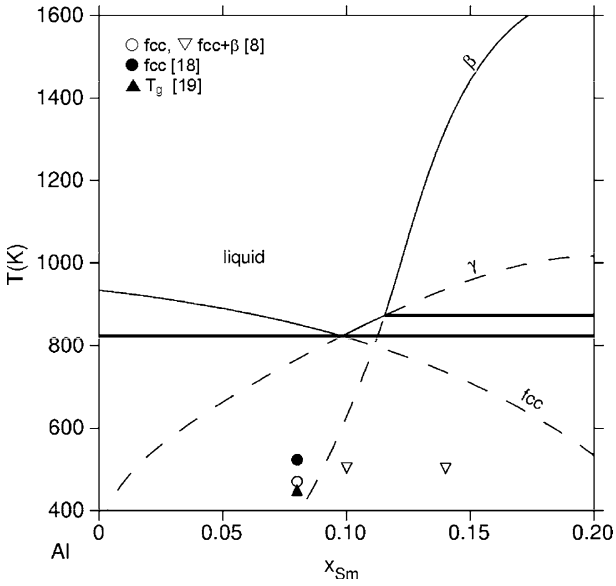

Fig. 7—Metastable liquidus curves for the indicated phases.

relevant two-phase mixtures. This figure supports our previous discussion concerning the metastable α liquidus, as shown in Figure 1(b). Moreover, from these calculations, we note that relaxation of either the liquid or the β phase to the α + L mixture would relieve a large fraction of the available free energy, leaving little driving force for further relaxation to either the δ + L or the δ + fcc two-phase mixture. While we have not addressed the kinetics of these decomposition reactions, this result is consistent with our experimental observation that very long annealing times are required for the α + L $\rightarrow$ δ + L transition, as indicated in Figures 2 and 4 and in Table II. In addition, the observed sluggishness of this weakly driven transformation naturally raises a question concerning the liquidus data reported by Saccone *et al.*[9] (Figure 1). Given that their data were obtained using continuous differential thermal analysis and that they did not specifically confirm the presence of either the δ or the α phase, we cannot rule out the possibility that their data represent the metastable α liquidus rather than the full equilibrium δ liquidus.

We now consider our results briefly with respect to observed devitrification paths in Al-Sm alloys. While the quantification of complex devitrification paths requires accurate thermodynamic descriptions and detailed analysis of the nucleation and growth kinetics pertaining to the relevant stable and metastable phases, we forego this comprehensive analysis here, and compare our results with experimental reports,[8,18,19] considering only the initial crystalline phases observed during devitrification treatments, as shown in Figure 7. This figure shows that reported devitrification occurs above T_g. Accordingly, we compare the observed crystallization with the relevant solid-liquid equilibria and note that the reported data are consistent with our fcc and β liquidus curves.

V. SUMMARY AND CONCLUSIONS

We offer the following key points from our analysis. (1) For the overall composition of Al_4Sm, liquid is stable above 1655 K, the β phase is stable from 1655 to 1333 K, the L + δ mixture is stable from 1333 to 919 K, and the fcc + δ mixture is stable below 919 K. (2) The orthorhombic intermetallic $Al_{11}Sm_3$-α and Al_4Sm-γ phases have no range of full stability, but are metastable down to 0 K, with respect to the Al(fcc) and Sm(rho) reference states. (3) The β phase may decompose catatectically to L + δ below 1333 K or to L + α below 1329 K. Alternatively, β may transform allotropically to α below 1135 K or to γ below 873 K, where the Al_4Sm composition is maintained. (4) The decomposition of the metastable α phase to either L + δ or to fcc + δ is only

weakly driven and, therefore, very sluggish. (5) The metastable phase diagram with extended fcc and β liquidus curves is consistent with experimental reports of initial crystallization behavior for the amorphous alloys.

ACKNOWLEDGMENTS

This work was performed within the Ames Laboratory Materials and Engineering Physics Program and was made possible by support from the Office of Basic Energy Science, Division of Materials Science, United States Department of Energy, under Contract No. W7405-Eng-82. The authors also thank Dr. A. Kracher for assistance with EPMA measurements.

REFERENCES

1. M.X. Quan, P. Haldar, J. Werth, and B.C. Giessen, *Rapidly Solidified Alloys and Their Mechanical and Magnetic Properties*, B.C. Giessen, D.E.P. Polk, A.I. Taub, eds., Materials Research Society, Boston, Massachusetts, 1985, vol. 2–4, pp. 299–04.
2. A. Inoue, T. Zhang, K. Kita, and T. Masumoto: *Mater. Trans., JIM*, 1989, vol. 30, pp. 870–77.
3. A. Inoue: *Progr. Mater. Sci.*, 1998, vol. 43, pp. 365–520.
4. S.C. Tjong and J.Q. Wang: *Z. Metallkd.*, 2001, vol. 92, pp. 610–16.
5. J.H. Perepezko, R.J. Hebert, and W.S. Tong: *Intermetallics*, 2002, vol. 10, pp. 1079–88.
6. J.H. Perepezko, R.J. Hebert, R.I. Wu, and G. Wilde: *J. Non-Cryst. Solids*, 2003, vol. 317, pp. 52–61.
7. K.H.J. Buschow and J.H.N. van Vucht: *Philips Res. Repts.*, 1965, vol. 20, pp. 15–22.
8. J.Q. Guo, K. Ohtera, K. Kita, J. Nagahora, and N.S. Kazama: *Mater. Lett.*, 1995, vol. 24, pp. 133–38.
9. A. Saccone, G. Cacciamani, D. Maccio, G. Borzone, and R. Ferro: *Intermetallics*, 1998, vol. 6, pp. 201–15.
10. A. Iandelli: *The Physical Chemistry of Metallic Solutions and Intermetallic Compounds*, National Physical Laboratory, Great Britain, Her Majesty's Stationery Office, London, 1959, vol. I.
11. H.J. Wernick and S. Geller: *Trans. Metall. Soc. AIME*, 1960, vol. 218, pp. 866–68.
12. F. Casteels: *J. Less-Common Met.*, 1967, vol. 12, pp. 210–20.
13. K.H.J. Buschow and J.H.N. van Vucht: *Philips Res. Repts.*, 1967, vol. 22, pp. 233–45.
14. A.H. Gomes de Mesquita and K.H.J. Buschow: *Acta Crystallogr.*, 1967, vol. 22, pp. 497–501.
15. K.A.J. Gschneidner and F.W. Calderwood: *Bull. Alloy Phase Diagrams*, 1989, vol. 10, pp. 37–39.
16. T.B. Massalski: *Binary Alloy Phase Diagrams*, ASM INTERNATIONAL, Materials Park, OH, 1990, pp. 213–14.
17. P. Rizzi, C. Antonione, M. Baricco, L. Battezzati, L. Armelao, E. Tondello, M. Fabrizio, and S. Daolio: *Nanostruct. Mater.*, 1998, vol. 10, pp. 767–76.
18. P. Rizzi, M. Baricco, S. Barace, and L. Battezzati: *Mater. Sci. Eng., A*, 2001, vols. 304–306, pp. 574–78.
19. G. Wilde, H. Sieber, and J.H. Perepezko: *J. Non-Cryst. Solids*, 1999, vol. 252, pp. 621–25.
20. J.H.N. van Vucht and K.H.J. Buschow: *Philips Res. Repts.*, 1964, vol. 19, pp. 319–22.
21. K.H.J. Buschow and A.S. Vandergoot: *J. Less-Common Metals*, 1971, vol. 24, pp. 117–20.
22. F. Casteels, P. Diels, and A. Cools: *J. Nucl. Mater.*, 1967, vol. 24, pp. 87–94.
23. O.V. Zhak, B.M. Stelmakhovych, and Y.B. Kuzma: *J. Alloy Compd.*, 1996, vol. 237, pp. 144–49.
24. MPC: *Materials Preparation Center*, Ames Laboratory, US DOE, Ames, IA.
25. G. Kresse and D. Joubert: *Phys. Rev. B*, 1999, vol. 59, pp. 1758–75.
26. D. Vanderbilt: *Phys. Rev. B*, 1990, vol. 41, pp. 7892–95.
27. J.P. Perdew, J.A. Chevary, S.H. Vosko, K.A. Jackson, M.R. Pederson, D.J. Singh, and C. Fiolhais: *Phys. Rev. B*, 1992, vol. 46, pp. 6671–87.
28. A.T. Dinsdale: *CALPHAD*, 1991, vol. 4, pp. 317–424.
29. S.H. Zhou and R.E. Napolitano: unpublished research.